Available online at www.sciencedirect.com
SCIENCE DIRECT®
Polymer 45 (2004) 1357–1364
polymer
www.elsevier.com/locate/polymer

Molecular dynamics modeling of polymer crystallization from the melt

Takashi Yamamoto*

Department of Physics, Biology, and Informatics, Faculty of Science, Yamaguchi University, Yamaguchi 753-8512, Japan

Received 3 February 2003; received in revised form 1 April 2003; accepted 2 April 2003

Abstract

Molecular pathways to polymer crystallization and the structures of crystal-melt interfaces are investigated by molecular dynamics simulation. We adopt a simplified molecular model for polymethylene-like chains; the chain is made of CH_2-like beads connected by harmonic springs, and the lowest energy conformation is a linear stretched sequence of the beads with slight bending stiffness being imposed. Two molecular systems are considered, one is made of 640 chains of C100 and the other is made of 64 chains of C1000, both being placed between two parallel substrates that represent the growth surfaces of the lamellae growing toward each other. The initial melt kept at a sufficiently high temperature above the melting point is rapidly cooled down to various crystallization temperatures, and the molecular processes of crystallization that follow are investigated. In both systems, we clearly observe the growth of stacked chain-folded lamellae from the substrates. The growing lamellae have a definite tapered shape, and they show marked thickening growth along the chain axis as well as usual growth perpendicular to it. The overall crystallization rate is found to be very sensitive to the crystallization temperature, showing an apparent maximum around 320–330 K for C100. We find that the lamellae do not grow keeping pace with each other but grow in independent rates especially at higher temperatures. We also examine the structures of the lateral growth surfaces and find that the growth surfaces are locally flat and the Kossel mechanism of crystal growth seems to be operative. In addition, the fold surfaces are found to be covered with relatively short chain-folds; at least about 60–70% of the folds are connecting the nearest or the next nearest neighbor crystalline stems. No appreciable bond orientational order is found in the undercooled melt of C100 and C1000.

Keywords: Molecular dynamics; Kossel mechanism; Polymer crystallization

1. Introduction

Molecular processes of linear polymers forming compact chain folded structures are of great interest common to polymer science and molecular biology. The polymer molecules form the folded structures induced by weak van der Waals attraction. However, the folding processes are hindered by strong excluded volume repulsion, which forbids the chain-crossings and leads to the specific topological constraints to the chain motions. The behavior of such complicated objects forming specific three-dimensional ordered structures poses a great challenge to molecular simulations.

Since the early discoveries of very thin lamellar crystals of polymers with remarkable chain folding, the polymer crystallization has attracted continuous attention of polymer scientists [1]. The understanding of detailed molecular mechanisms of the polymer crystallization is really indispensable to many important technologies of designing favorable microscopic and macroscopic structures of crystalline polymers.

Most of the experimental data obtained so far have been successfully interpreted by use of the Lauritzen–Hoffman (LH) theory of secondary-nucleation; the theory was constructed on bold simplifying assumptions for the molecular processes involved [2]. Despite the great success of the LH-theory, the molecular mechanism of polymer crystallization is still a very controversial problem. For example, the diverse molecular images of the fold surfaces ranging from the sharp adjacent-reentry model to the random switchboard model, and the possible presence of orientational order in the undercooled melt before the onset of crystallization, are still very controversial. Many researchers have been trying to get more detailed molecular pictures or to construct completely new scenarios [3–11]. The largest underlying difficulty is that most of the experimental data obtained could be explained by any of

* *E-mail address:* yamamoto@mms.sci.yamaguchi-u.ac.jp (T.Yamamoto).

0032-3861/$ - see front matter © 2003 Elsevier Ltd. All rights reserved.
doi:10.1016/j.polymer.2003.04.006

these molecular level scenarios; we still do not have any conclusive experimental evidence to choose one of them. The difficulty seems to be deeply rooted in our experimental inability to observe the molecular process of polymer crystallization directly.

In order to overcome these experimental difficulties, many molecular simulation studies are emerging. The potential power to directly reproduce the polymer crystallization thereby enabling detailed inspections of the chain folding processes is expected to give decisive answers to the long-standing arguments for a half century.

We started our computer simulation studies on polymer crystallization with Monte Carlo studies on crystal-melt interfaces of *n*-alkanes [12,13]. Recently we have been trying to simulate the molecular processes of long chain polymers being adsorbed to the growth front followed by chain-folding, which are the most important elementary processes of the polymer crystal growth [14–16]. We have also reported on the spontaneous formation of the fiber structure from an oriented amorphous state [17]. In our previous study [18], we have extended our former molecular dynamics (MD) simulation of melt crystallization to a much larger system of 64,000 atoms made of 640 polymethylene-like molecules C100. We have observed there the steady-state growth of the chain folded lamellae and have discussed the lamella growth rate vs. crystallization temperature T_c. We have also examined the molecular trajectories at the growth front. In addition, we have reported that no appreciable orientational order was noticed in the melt of C100. Many efforts in the similar directions have been made with great success [19–28], and the science of polymer crystallization is now led to a new stage of development. In this paper, we present detailed analyses of our MD simulation data for C100. We also show our recent simulations of the crystallization of much longer chains C1000.

2. Model and method

In this paper, we consider two systems of polymethylene-like molecules, one made of 640 chains of C100, and the other 64 chains of C1000; the total number of atoms are both 64,000. Since the crystallization in multiple chain systems is very sluggish, we must accelerate crystallization. We therefore adopt a simplified molecular model [16,18]. Our model molecule is a polymethylene-like chain made of beads of mass 14 connected by harmonic springs with the potential

$$V_b = \frac{1}{2}k_b(r - r_0)^2 \tag{1}$$

where r is the C–C bond length, r_0, the equilibrium bond length of 0.154 nm, and k_b is the spring constant. We previously found that fully flexible chains show extremely slow crystallization from the melt, so we make the chains slightly stiffer by adding an extra potential energy for the bond angle bending

$$V_\theta = a - b(\cos\theta - \cos\theta_0) + d(\cos\theta - \cos\theta_0)^3 \tag{2}$$

where θ is the C–C–C bond angle, and θ_0 is taken as 108.78°. This potential was constructed to give the lowest energy of 0.0 kcal at $\theta = 180°$, a local minimum of 0.6 kcal at $\theta = 90°$ (90° kink), and an energy barrier of about 3.0 kcal at an intermediate angle $\theta = 130°$; the values of the parameters a, b, and d were selected to model the flexibility (*gauche* bond generation) of the polymethylene chain (Table 1). Since the lowest energy conformation is a linear sequence of atoms with bond angle $\theta = 180°$, we do not consider the energy of internal rotation of the bonds. Our model molecule prefers to take a straight conformation, and this facilitates the chain diffusion along the chain axis as well as transverse to it. Between atoms more than two bonds apart, and those of different chains, we assume usual van der Waals interactions of Lennard–Jones type

$$V_{vdW} = 4\varepsilon\left[\left(\frac{\sigma}{r}\right)^{12} - \left(\frac{\sigma}{r}\right)^{6}\right] \tag{3}$$

where the van der Waals parameters ε and σ adopted are the same as those of the united atom model of polymethylene (Table 1).

It was shown in our previous reports [16,18] that the chains, especially relatively short chains free from boundary effects, take ideal random-coil conformation. The characteristic ratio $\langle R_N^2\rangle/Nl^2$, where l is the bond length and N is the degree of polymerization, was about 7.8, the value very close to the experimental ones of about 6.7 for polyethylene [29,30]. Present simplified polymer model is thus considered to mimic the flexibility of polymethylene chains very well.

The polymer melt is sandwiched between two parallel substrates that model the growth surfaces of real polyethylene single crystals (Fig. 1). The substrates here correspond to the hexagonal (100) faces of lamellae made up of the closely packed bead-spring chains running along

Table 1
List of parameters and their values

Parameter	Values	Units
m	14×10^{-3}	kg/mol
k_b	3.5×10^{25}	J/m^2 mol
r_0	0.154	nm
a	7.440×10^3	J/mol
b	2.297×10^4	J/mol
d	7.386×10^4	J/mol
θ_0	108.78	°
ε	598.64	J/mol
σ	0.392	nm
λ	0.433	nm
d_s	0.375	nm
Z_c	0.229	nm

σ is a unit length in reduced unit.

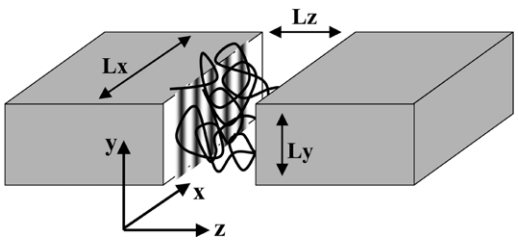

Fig. 1. Schematic picture of the simulated system. Polymer chains are sandwiched between parallel substrates that correspond to the growth surfaces of two lamellae; the substrate lamellae are also made of the same model polymer chains. The z-axis is taken normal to the substrate, while the y-axis is along the chain direction of the substrate crystals.

the y-axis. On the other hand, we adopted free boundary conditions in the x- and y-axis directions in order to reduce computational load and to avoid interactions of the chains with their periodic images. The size of the present system is 11.8 nm in each direction ($L_x = L_y = L_z = 11.8$ nm), and the resulting average density is about 0.86 (g/cm^3).

The interaction energies between each polymer atom and all the substrate atoms can be efficiently summed up into Fourier series by the method of Steele [31]. In the present work, we use the lowest order Fourier component only [16,18]. The potential energy from the substrate is thus given as follows

$$V_{\mathrm{sub}}(x,y,z) = V_0(z) + V_1(z)\cos(2\pi\frac{x}{\lambda}) \tag{4}$$

$$V_0(z) = \frac{2\pi\varepsilon}{\lambda r_0}\left(\frac{2\sigma^{12}}{5z^{10}} - \frac{\sigma^6}{z^4} - \frac{\sigma^6}{3d_s(z+z_c)^3}\right) \tag{5}$$

$$V_1(z) = \frac{4\pi\varepsilon}{\lambda r_0}\left(\frac{\sigma^{12}\pi^5}{30(z\lambda)^5}K_5\left(\frac{2\pi z}{\lambda}\right) - \frac{2\sigma^6\pi^2}{(z\lambda)^2}K_2\left(\frac{2\pi z}{\lambda}\right)\right) \tag{6}$$

where K_n is the modified Bessel function, z, the distance from the substrate, λ, the inter-chain separation on the substrate, r_0, the bond length, and $z_c = 0.61d_s$ is a correction factor with d_s being the lattice spacing of the substrate plane [31]. The parameter values used are listed in Table 1.

The approximate melting temperature T_m of the present system was estimated to be around 400 K [16,18]. We first prepare an equilibrium melt at 500 K sufficiently higher than T_m. Then, we quench the melt down to various crystallization temperatures T_c and monitor in detail the molecular processes of crystallization that follow. We adopt a simple integration scheme, the leap-frog method, with the temperature control by rescaling velocities every 10 integration steps, where one integration step is about 3.2 fs.

3. Results and discussions

3.1. Growth and melting of the chain folded lamellae of C100

3.1.1. Stationary growth of the chain folded lamellae

We first show a typical snapshot (Fig. 2) of the system of C100 at 12.8 ns after quenching down to 350 K, which clearly shows the growth of stacked lamellae from both side substrates. In order to demarcate the crystalline regions, we here define the crystal domains as being made of well-aligned and closely-packed C–C bonds. We first pick up C–C bonds that are nearly parallel to the y-axis with angles θ less than 20° (Fig. 3(a)). Out of these candidate bonds, we consider those bonds that have at least three neighbors as crystalline bonds (Fig. 3(b)), where we consider the bonds are neighboring when the vector $\mathbf{r}$ connecting the centers of the bonds satisfies $0.7\sigma < \sqrt{r_x^2 + r_z^2} < 1.3\sigma$ and $|r_y| < r_0/2$ (Fig. 3(a)).

Fig. 4 shows a typical growth process at 330 K of the crystal domains defined above. The lower pictures viewed along the y-axis show the hexagonal packing of the chains, while the upper pictures viewed along the x-axis demonstrate the growth of stacked lamellae. All the lamellae have a marked tapered shape, which is preserved until they collide with those growing from the opposite substrate. The lamellae grown from the opposite substrates make collision around 10 ns and merge into larger lamellae around 20 ns. Each lamella is found to show the thickening growth along the chain axis as well as the usual lamella growth perpendicular to it.

Fig. 5 shows the increases in crystallinity χ_c, the fraction of atoms that belong to the crystal domains, at various crystallization temperatures T_c. At any temperature, the crystallinity initially increases up to around 10%, which is found due to the surface layering in the melt near the solid boundaries [16]. After the initial increases, χ_c shows approximately linear increases, up to about 10 ns, due to the usual growth of lamellae until it begins to slow down.

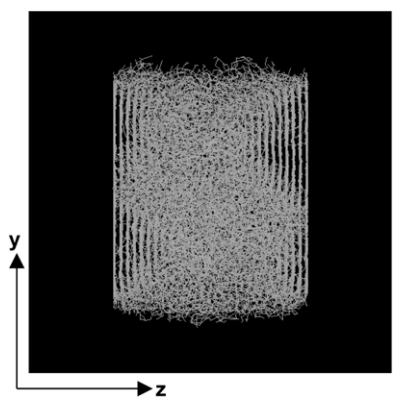

Fig. 2. A representative snapshot, obtained at 12.8 ns after quenching to 350 K, of the system made of 640 chains of C100. We readily notice crystalline domains growing toward each other from both the substrates.

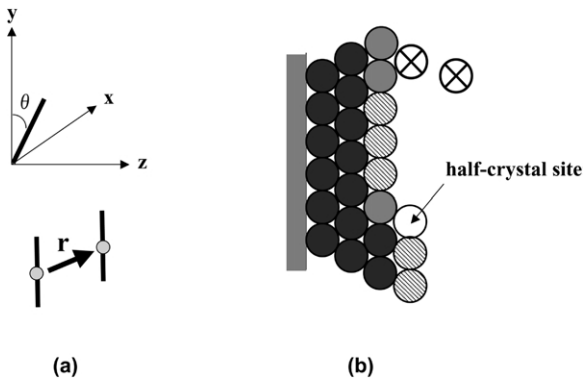

Fig. 3. The bonds that form crystalline domains nearly parallel to the y-axis with angle θ less than 20°. Furthermore, the bonds must have at least three neighbors that satisfy $0.7\sigma < \sqrt{r_x^2 + r_z^2} < 1.3\sigma$ and $|r_y| < r_0/2$. Note in (b) that the crystalline stems deep inside the crystal (black spheres) have six neighbors, while those on the free surfaces (hatched spheres) have four neighbors. The stems at the half-crystal site, or at the kink site (white sphere) have three neighbors. The single stem attached on the free surface and that floating in the melt phase (spheres with a cross) have less than three neighbors.

The growth rate saturation may be due to lamella collisions but can also be due to other factors yet unknown.

The crystallization rate sensitively depends on T_c. The crystallization is very slow at higher temperatures around T_m; it is actually too slow to be detected around $T_c =$ 370–390 K. The crystallization rate increases with decreasing temperature and shows an apparent maximum around $T_c = 330$–320 K. At 300 K we previously found that the crystallization rate again decreases, which was considered to be an indication of the restricted chain mobility at lower temperatures [16].

Fig. 6(a) and (b) shows the growth of each lamella size, the number of atoms within each lamella at 330 and 350 K, respectively. It clearly shows that the lamellae do not always grow keeping the pace with each other. The growth rate irregularity is especially marked at the higher temperature 350 K, where the four lamellae grow at quite distinct rates. These anomalous growth rates may be simply due to statistical fluctuations in small systems. But similar

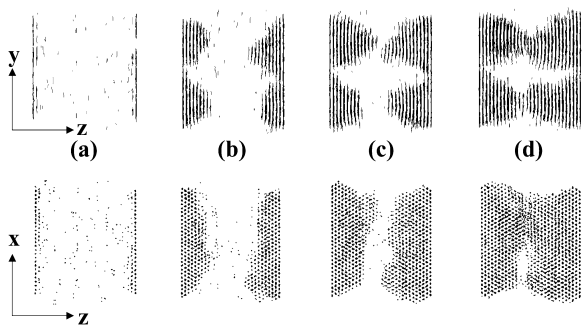

Fig. 4. Three-dimensional pictures of growing lamellae at 330 K, viewed along the x-axis (above), and viewed along the y-axis (below); (a) at 0.128 ns, (b) at 6.4 ns, (c) at 12.8 ns, and (d) at 19.2 ns. We notice the tapered growth fronts and their advances in the normal (the z-axis) direction together with the lamella thickening along the chain axis (the y-axis direction).

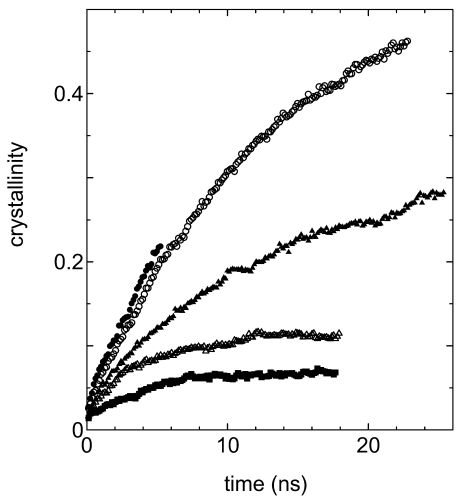

Fig. 5. Increases in the overall crystallinity with time, at 390 K (■), at 370 K (△), at 350 K (▲), at 330 K (○), and at 320 K (●). The crystallinity is defined as the fraction of chain atoms that belong to the ordered domains.

incoherent lamella growth in the shish-kebab structure was observed by recent AFM investigation [32]. We suspect some unknown but very important controlling factors, such as chain entanglements in the melt, are operative.

3.1.2. Melting of lamellae and their equilibrium shape

Marked tapered shapes are observed in the growing lamellae. Similar tapered edges, though of much smaller angles, are also observed in case of crystallization into highly mobile phases such as the high-pressure phase of polyethylene [6]. The growth of very thin polymer lamellae is usually governed by kinetic factors [1–3]. So, we initially considered the tapered shape was also a kinetic form, and we examined how the tapered edges change their shapes during melting or by holding near the melting temperature. Fig. 7(a)–(d) shows the melting of the lamellae at 380 K by quickly raising the temperature from 330 K (the initial stet is that of Fig. 3(c)). Quite unexpectedly, the lamellae showed just a reverse process, the rapid retreat of the growth fronts maintaining the tapered shapes. Furthermore, when the same initial lamellae were quickly heated and held at 360 K, the lamellae showed neither growth nor melting at least within 10 ns, but again the tapered shape of the lamellae was preserved at least up to about 9 ns (Fig. 7(e)–(h)). All these observations suggest that the tapered shape is not a kinetic form but rather an equilibrium form.

The tapered shape of the lamella indicates the preference of the fold surfaces to have an inclination from the chain-axis normal. It is well known that the density difference between the amorphous and the crystalline phases often results in the chain tilting. We made a rough estimation of the tilt angle by assuming that all the crystalline stems emanating from the fold surface join to form the amorphous phase; the fold loops are assumed not so tight even if the chains fold back to nearer positions. The densities of the crystalline and the amorphous phases are approximately

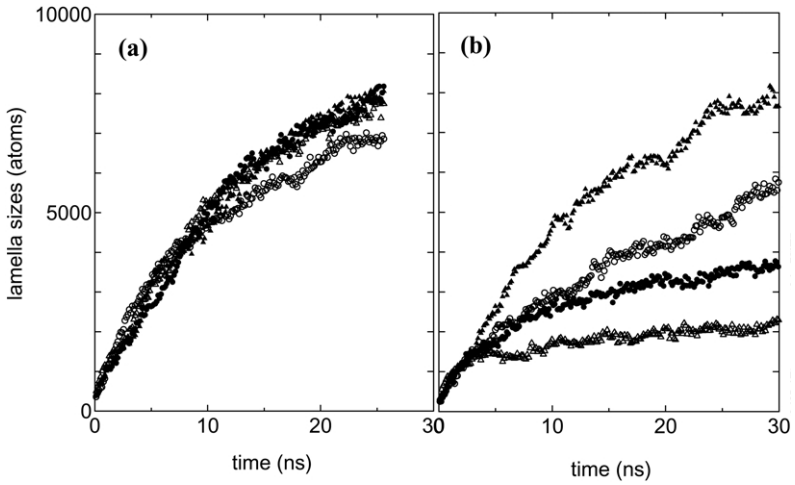

Fig. 6. Growth of each lamella, the number of atoms in the lamella, vs. time, (a) at 330 K and (b) at 350 K. Please notice that the lamellae show quite different growth rates especially at higher temperatures.

0.86 (g/cm^3) and 0.93 (g/cm^3), respectively, and then the resulting tilt angle is estimated to be about 21°, which is rather near to that observed by the present simulation. But very recently Dr Toda suggested to me that there can be another equilibrium explanation to the tapered shape, the key of which is a pining effect proposed by late Sadler [33]. But here we do not want to dwell on detailed arguments.

3.1.3. Structures of the fold- and growth-surfaces

The structure of fold surfaces has been one of the most controversial problems since the finding of the chain folded crystals. It is very interesting to examine the fold structures that the MD simulation predicts. Fig. 8(a) and (b) shows pictures of the fold loops and of the cilium, respectively, emanating from a lamella at 330 K after 19.2 ns (Fig. 4(d)). We can notice that most of the fold loops near the substrate are rather short. Looser and longer loops and abundant cilium at the middle of the MD cell is obviously because the crystallization is not completed and many amorphous segments are remaining to be crystallized around the center of the MD cell even after 19.2 ns.

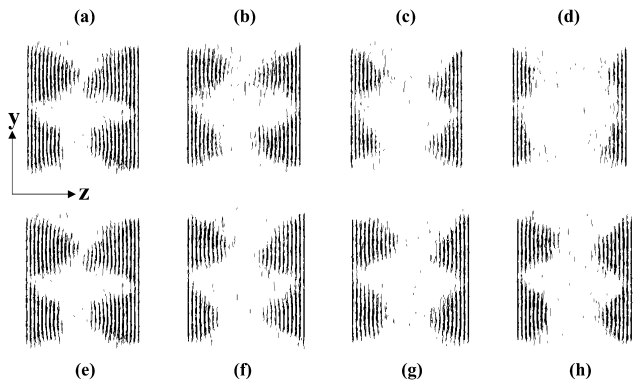

Fig. 7. Changes in the lamella profiles viewed along the x-axis, during melting at 380 K (above), and during holding at 360 K (below); (a) at 0.0 ns, (b) at 0.128 ns, (c) at 0.64 ns, (d) at 1.28 ns, (e) at 0.0 ns, (f) at 2.56 ns, (g) at 6.4 ns, and (h) at 8.96 ns. We can notice that the tapered growth fronts retreat at 380 K, and stand stationary at 360 K, maintaining the tapered profile at the edges.

Though the obtained lamellae are still incomplete even after 20 ns, we have analyzed the statistical distribution of the fold loops. In order to examine the degree of chain folding into the nearest and the next nearest neighbor stems, we have measured the inter-stem distances (the $x-z$ plane projection) connected by the loops, that are the projected end-to-end distances of the fold loops. The radial distribution of the inter-stem vectors projected onto the $x-z$ plane (Fig. 9) shows that most of the fold loops, of about 60–70%, are connecting the nearest or the second and third nearest neighbor stems of the hexagonal lattice; the first peak corresponds to the folds connecting the nearest neighbor stems (⟨100⟩ and ⟨110⟩ folds), while the second peak comes from those connecting the second and the third nearest stems (⟨210⟩ and ⟨200⟩ folds). The preference of the short folds would become even greater in systems with higher crystallinity after much longer simulation times. Detailed statistics of the fold structure is a very important subject of research, and indeed equilibrium Monte Carlo investigations were proved to give important information [34]. Since our present lamellae are still growing with many melt chains waiting to be crystallized, however, full statistical

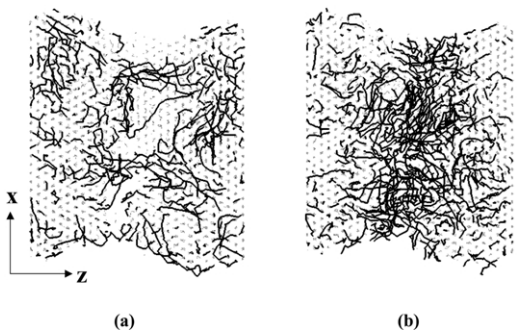

Fig. 8. Polymer segments forming (a) fold loops and (b) cilia, which are emanating from upper two lamellae in Fig. 4(d).

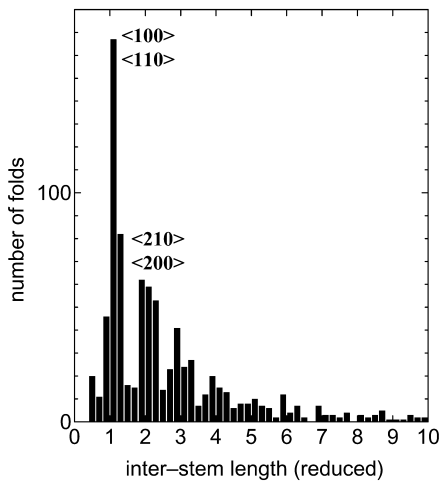

Fig. 9. Radial distribution of inter-stem vectors, in Fig. 8, connecting stems linked by loops. The folds connecting stems separated by the ⟨100⟩, ⟨110⟩, ⟨210⟩, and ⟨200⟩ hexagonal lattice vectors are dominant.

analyses of the fold structure will remain as our future projects.

The structure of the lateral growth surfaces, whether rough or smooth, is of prime importance in constructing the molecular theory of crystal growth. Since the crystal-melt interfaces are extremely difficult to investigate by experiments, we here examine the structure of the growth surfaces and the molecular process of crystal-stem additions onto it. Fig. 10 shows the hexagonal chain packing of the growing lamellae, the two lamellae in the lower half of Fig. 4(b), viewed along the chain axis. Relatively smooth surfaces are observed, though not so wide, and they correspond to the {100} planes of the hexagonal lattice. The stepwise addition

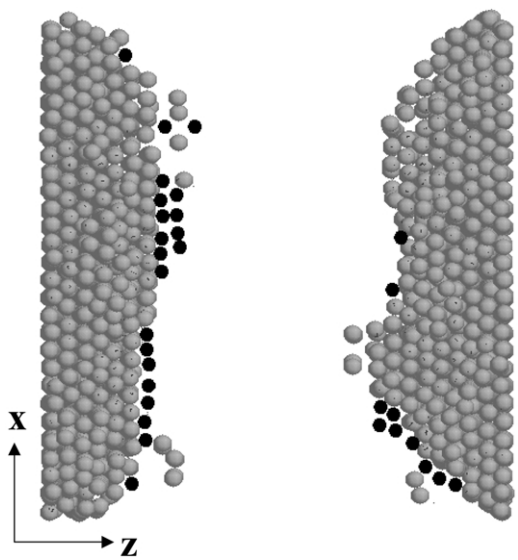

Fig. 10. Mode of chain packing at 330 K at 6.4 ns (grey spheres). The crystalline lamellae are found to have rather flat {100} surfaces. Also shown are newly added stems (black spheres) during the next 0.128 ns of simulation.

of the crystalline stems onto the plane surface, just like the Kossel mechanism in the crystal growth of simple molecules, is thus strongly suggested. We can verify this idea by monitoring the stem adsorption processes. Also shown in Fig. 10 are the positions of crystalline stems that newly adhered onto the surface during the next 0.128 ns (black spheres). The additions of new crystalline stems are found mostly along the low index {100} surfaces or at the kink sites.

3.2. Crystallization of much longer chains C1000 from the melt

The discussions were so far concerned with relatively short chains C100. We want to extend our simulations into much longer chain systems. We here present our recent simulations, though still preliminary, on 10 times longer chains C1000. However, we must here begin with a caveat. Polymer chains in the fully equilibrated melt should be ideal Gaussian random coils, which have spatial dimensions proportional to the square root of their degrees of polymerization [35]. The end-to-end distance of C1000 in the melt is thus expected to have about three times larger than that of C100. We have previously confirmed that the present MD-cell size was large enough for the chains C100 to show ideal Gaussian dimension [16]. In order to give the chains C1000 as large a space, we must adopt an MD-cell whose linear dimension is three times larger containing as many as two million of atoms. Therefore, we must be here contented in dealing with a system of the same MD-cell size as that of C100, 30σ cube, containing 64 chains of C1000; we must expect serious size effects in the crystallization processes.

3.2.1. Structural characterization of the melt above T_m

The density of the melt is readily equilibrated, while the equilibration of the chain conformation needs much longer time. The chain conformation, the degree of chain extension, in the melt is well characterized by the following

$$R_n^2 = \langle (r_{n+m} - r_m)^2 \rangle$$

which represents the average inter-atomic distance n-atoms separated along the chain. If the chain is Gaussian random coil, this R_n^2 should be proportional to n. Fig. 11 shows the R_n^2 calculated in the melt, both for C100 and C1000. In case of C100, R_n^2 shows strictly linear increase with n, which clearly indicate the chains in the melt have ideal Gaussian conformation as already described in our previous paper [16]. In case of C1000, on the contrary, R_n^2 follows the linear increase only in very small n range, and it soon come to show remarkable deviation. The deviation, the non-ideal chain conformation, will undoubtedly come from finite size effect of the MD cell. In the discussions that follow, we must always be prepared to make allowance for the effect that the chains are not fully entangled in the melt.

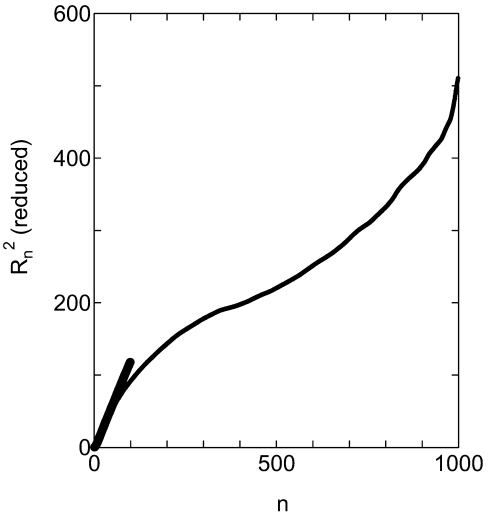

Fig. 11. The chain conformation in the melt. The averaged square interatomic distances, R_n^2, between atoms n bond apart along the chains are plotted vs. n, both in C100 (a thick line) and in C1000 (a thin line). An ideal random coil conformation is readily noticed for C100, while C1000 shows marked deviations except at very small n.

3.2.2. Crystallization from the melt

The initial melt of C1000 was cooled down to various crystallization temperatures T_c. Typical developments of crystal domains at 350 and 370 K are shown in Fig. 12; here again the lamellae have the marked tapered shape. Quite surprising is that the crystallization of C1000 is rather fast in spite of much longer chain dimension. The growth of lamellae of C1000 at the high temperature of 370 K, where C100 did not show any appreciable growth, will be an indication of the molecular weight effect.

Fig. 13 shows typical molecular trajectories at 370 K of a chain selected at random. When a sufficiently long random coil chain approaches the growth front, it is quite reasonable to consider that a part of the chain is pulled out and adheres to the growth front resulting in a hairpin. In Fig. 13(a), a loop is attracted to the growth surface and a hairpin is formed (Fig. 13(b)). The hairpin climbs down the growth

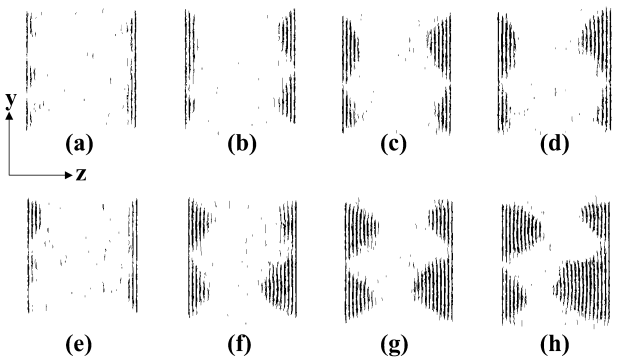

Fig. 12. Three-dimensional pictures of growing lamellae of C1000 at 370 K (a) at 0.128 ns, (b) at 6.4 ns, (c) at 12.8 ns, and (d) at 19.2 ns (above), and at 350 K (e) at 1.28 ns, (f) at 6.4 ns, (g) at 12.8 ns, and (h) at 24.2 ns (below), all viewed along the x-axis. We again notice the tapered growth fronts and their advances in the normal (the z-axis) direction together with the lamella thickening along the chain axis (the y-axis direction).

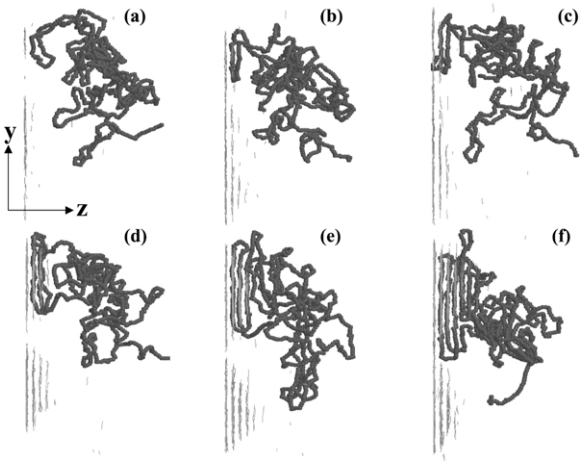

Fig. 13. Molecular trajectories of a crystallizing chain (thick line) selected at random from 64 chains during crystallization at 370 K; (a) at 0.128 ns, (b) at 0.64 ns, (c) at 1.28 ns, (d) at 2.56 ns, (e) at 6.40 ns, and (f) at 12.8 ns. Also shown are the growing crystalline domains of Fig. 12 (thin parallel lines). Pictures are all side view along the x-axis.

surface to complete the crystalline stems, followed by further folding of the tails that are connected to the hairpin. As an initial step of the surface secondary nucleation, the significance of such a stem pair or a hairpin is already suggested in previous papers [14,23,25,26]. Here again, we have arrived at a similar conclusion.

We examined the fold statistics in this C1000 system also. The distribution of the inter-stem vectors connecting stems linked by the loops, and their radial distribution function again indicated that about 60–70% of the folds are short loops connecting the nearest or the second and third nearest stems, though the crystallization was not complete even at 350 K.

The expected local order in the undercooled melt and its role in polymer crystallization have been the subjects of long-standing arguments [8,9]. In our previous study [18], we reported that we could not detect any appreciable orientational order in the melt of C100. We here studied the same local order $P(r)$, the degree of bond orientation as a function of position $\mathbf{r}$ in the undercooled melt of C1000

$$P(r) = \langle (3\cos^2\theta_{ij} - 1)/2 \rangle$$

where θ_{ij} is an angle between the ith and the jth C–C bonds within a small cubic box, located at $\mathbf{r}$, of size 3σ containing approximately 60 bonds. Fig. 14 shows again that no appreciable order is found in the undercooled melt.

4. Conclusions

The microscopic processes of polymer crystal growth were investigated by MD simulation, in the systems of relatively short C100 chains and sufficiently long C1000 chains. In both systems, we observed the growth of chain folded lamellae that have marked tapered edges; the

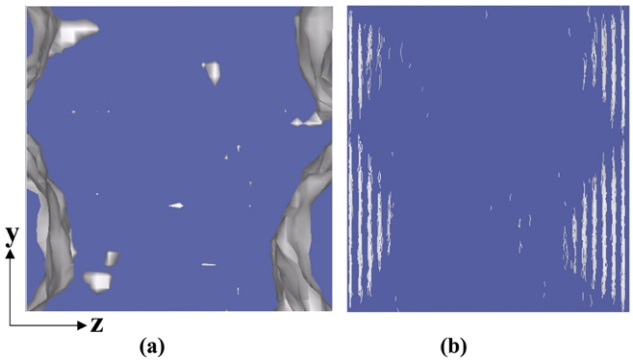

Fig. 14. Local bond orientational order and the growth of lamellae after 17.92 ns at 370 K. Equi-order parameter surfaces for $P = 0.3$ (a) show nice correspondence with the crystalline domains (b). Clearly (a) shows that no special bond orientational order is found in the isotropic melt region.

lamellae showed thickening growth along the chain axis as well as usual growth perpendicular to it. The crystallization was found to be very sensitive to the crystallization temperature, and the crystals nearly stopped growing around 360–370 K in C100 and around slightly higher temperatures in C1000. The inspection of the growth of each lamella showed that the lamellae do not always grow in concert, especially at higher temperatures near T_m.

We also found that the lateral growth surfaces are rather flat locally, in spite of their crystal-melt interfaces, and the molecular process assumed in the Kossel mechanism seems to be operative in polymer crystals also. In addition, the fold surfaces were found to be covered with relatively short chain folds, at least about 60–70% of which are connecting the nearest or the second and third nearest neighbor crystalline stems. Last, but not the least, our computer simulation did not indicate any sign of local order in the chain orientation within the undercooled melt of both C100 and C1000.

Acknowledgements

The present work was supported by the Grant-in-Aid of Scientific Research on Priority Areas, 'Mechanism of Polymer Crystallization' (No. 12127206), from the Ministry of Education, Science, and Culture, Japan.

References

[1] Wunderlich B, Macromolecular physics, vol. 2. New York: Academic; 1976.
[2] Hoffman JD, Miller RL. Polymer 1997;38:3151.
[3] Armistead K, Goldbeck-Wood G. Adv Polym Sci 1992;100:219.
[4] Point JJ. Macromolecules 1979;12:770.
[5] Sadler DM, Gilmer GM. Polymer 1984;25:1446.
[6] Hokosaka M. Polymer 1990;31:458.
[7] Keller A, Hikosaka M, Rastogi S, Toda A, Barham PJ, Goldbeck-Wood G. J Mater Sci 1994;29:2579.
[8] Strobl G. Eur Phys J E 2000;3:165.
[9] Imai M, Mori K, Mizukami T, Kaji K, Kanaya T. Polymer 1992;33:4451.
[10] Tashiro K, Imanishi K, Izumi Y, Kobayashi M, Kobayashi K, Satoh M, Stein R. Macromolecules 1995;28:8477.
[11] Fukao K, Miyamoto Y. Phys Rev Lett 1997;79:4613.
[12] Yamamoto T, Hikosaka M, Takahashi N. Macromolecules 1994;27:1466.
[13] Yamamoto T. J Chem Soc, Faraday Trans 1995;91:2559.
[14] Yamamoto T. J Chem Phys 1997;107:2653.
[15] Yamamoto T. J Chem Phys 1998;109:4638.
[16] Yamamoto T. J Chem Phys 2001;115:8675.
[17] Koyama A, Yamamoto T, Fukao K, Miyamoto Y. Phys Rev E 2002;65:050801.
[18] Yamamoto T. J Macromol Sci 2003; in press.
[19] Kavassalis TA, Sandararajan PR. Macromolecules 1993;26:4144.
[20] Fujiwara S, Sato T. J Chem Phys 1997;107:613.
[21] Chen CM, Higgs PG. J Chem Phys 1998;108:4305.
[22] Liu C, Muthukumar M. J Chem Phys 1998;109:2536.
[23] Doye JP, Frenkel D. J Chem Phys 1998;109:10033.
[24] Doye JP, Frenkel D. J Chem Phys 1999;110:2692.
[25] Welch P, Muthukumar M. Phys Rev Lett 2001;87:218302.
[26] Meyer H, Mueller-Plathe F. J Chem Phys 2001;115:7807.
[27] Meyer H, Mueller-Plathe F. Macromolecules 2002;35:1241.
[28] Waheed N, Lavine MS, Rutledge G. J Chem Phys 2002;116:2301.
[29] Lieser G, Fisher EW, Ibel K. J Polym Sci, Polym Lett Ed 1975;13:39.
[30] Brandrup J, Immergut EH, Grulke EA, editors. Polymer handbook. New York: Wiley; 1999.
[31] Steele WA. Surf Sci 1973;36:317.
[32] Hobbs JK, Miles MJ. Macromolecules 2001;34:353.
[33] Toda A. Private communication.
[34] Gautam S, Balijepalli S, Rutledge GC. Macromolecules 2000;37:9136.
[35] de Gennes P-G. Scaling concept in polymer physics. Ithaca: Cornell University Press; 1979.